scientific reports

Check for updates

OPEN

Identification of mitochondria-related biomarkers for acute respiratory distress syndrome

Huang Hongyuan[1,2,5], Chen Mengchi[3,5], Liang Yingying[1], Zheng Xiaowen[1], Huang Qiaojuan[1] & Liu Jianghua[1,4]✉

Mitochondria-related genes (MRGs) are considered screening MRGs as biomarkers for important therapeutic targets, but their role in acute respiratory distress syndrome (ARDS) remains unclear. This study aimed to identify MRGs-related biomarkers for ARDS. Intersection of 2030 MRGs with 343 differentially expressed genes (DEGs) between sepsis-non-ARDS and sepsis-ARDS group yielded 20 MRGs-related DEGs enriched in mitochondrion-related pathways. Monocytes, T cells, natural killer (NK) T cells, NK cells, and innate lymphoid cells (ILCs) were screened as candidate key cell types. SLC2A1 and IFI27 were defined as biomarkers; naive B cells, resting NK cells, and naive CD4 T cells, as differential immune cells; and monocytes, as the key cell type, subdivided into the CD14 and CD16 subtypes. The sepsis-ARDS group exhibited enhanced CD14 Mono and B cells compared with the sepsis-non-ARDS group and CD16 had a higher percentage and score in the G2/M and S phases than CD14. IFI27 and SLC2A1 were mainly expressed differently in the CD14 monocytes in ARDS, and their mRNA expression levels in peripheral blood of the sepsis patients was upregulated compared with those of the healthy controls. Thus, our findings demonstrate that SLC2A1 and IFI27 represent novel MRGs-related diagnostic biomarkers for ARDS, providing theoretical references for its treatment.

Keywords Acute respiratory distress syndrome, Mitochondria, Single-cell analysis, SLC2A1, IFI27

Abbreviations

ARDS	Acute respiratory distress syndrome
ATP	Adenosine triphosphate
ALI	Acute lung injury
ANN	Artificial neural network
AT2	Type II alveolar epithelial cells
BMI1	B cell specific Moloney murine leukemia virus integration site 1
BP	Biological processes
DEGs	Differentially expressed genes
EV71	Induced by enterovirus 71
GSVA	Gene set variation analysis
GGI	Gene-gene interaction
GEO	Gene Expression Omnibus
GSEA	Gene set enrichment analysis
HFMD	Hand, foot and mouth disease
KEGG	Kyoto Encyclopedia of Genes and Genomes
MRGs	Mitochondria-related genes
MF	Molecular function
NOX4	NADPH oxidase 4
PBMC	Peripheral blood mononuclear cell
PCA	Principal component analysis
PC	Principal component
PBMC	Peripheral blood mononuclear cells

[1]The Second Affiliated Hospital of Guangxi Medical University, Nanning 530000, Guangxi, China. [2]The Affiliated Tumor Hospital of Guangxi Medical University, Nanning 530000, Guangxi, China. [3]The Third Affiliated Hospital of Sun Yat-sen University, Guangzhou 510000, Guangdong, China. [4]School of Nursing, Guangxi Medical University, Nanning 530000, Guangxi, China. [5]Huang Hongyuan and Chen Mengchi contributed equally to this work. ✉email: jianghualiu0107@163.com

qRT-PCR	Quantitative reverse transcription polymerase chain reaction
ROC	Receiver operating characteristic
scRNA-Seq	Single Cell RNA Sequencing
TFs	Transcription factors

Acute respiratory distress syndrome (ARDS, for all abbreviations and their meanings, see Table 1) is a severe and life-threatening condition marked by acute hypoxic respiratory insufficiency. The core pathology of this disease involves the injury of alveolar epithelial cells and vascular endothelial cells, resulting in pulmonary edema. This damage and fluid buildup significantly impair the patient's respiratory function, ultimately contributing to the high morbidity and mortality associated with ARDS[1]. A large observational study of 459 hospital intensive care units (ICU) showed that 10.4% of the ICU patients had ARDS, while up to 23.4% of the ICU patients receiving mechanical ventilation had ARDS. However, the diagnosis of ARDS cases was often delayed, and their identification rate was low[2]. Thus, the ADS in-hospital mortality rate is as high as 35%–45%[3]. The current treatments for ARDS mainly include intubation or mechanical ventilation, inflammation management with corticosteroids, fluid management, and supportive care[4]. However, their therapeutic effects are poor, and their prognostic effects are lower than expected; thus, ARDS-specific treatments still need to be improved[5]. Recognizing ARDS as early as possible is critical to save patients' lives through timely and appropriate ventilation. However, early detection and treatment of ARDS require a deeper understanding of the cellular and molecular processes underlying the disease, which could facilitate the development of biomarkers and new therapies.

Mitochondria-related genes (MRGs) hold great promise as biomarkers for the diagnosis of ARDS. Mitochondria, which originated from an α-proteobacterium engulfed by eukaryotic host cells through endosymbiosis, generate adenosine triphosphate (ATP) containing high-energy phosphate bonds that provides energy for other intracellular reactions[6]. However, this process makes the mitochondria a significant site for generating reactive oxygen species (ROS) due to the abnormal release of free electrons, making the mitochondria a significant site for generating reactive oxygen species[6]. In many chronic inflammatory and infectious diseases, the mitochondrial network is destroyed, leading to excessive ROS production that contributes to improper immune responses, tissue damage, and ultimately, organ failure. Therefore, targeted control of mitochondrial dysfunction and oxidative stress could be a promising strategy for ARDS management.

Mitochondrial dysfunction in ARDS can manifest though various mechanisms, including mitochondrial DNA mutations[7], changes in membrane potential changes[8], and disruptions in mitochondrial dynamics[9,10]. These alterations could initiate or amplify inflammation, thereby playing a significant role in the development of ARDS. Research has shown that silencing the B cell-specific Moloney murine leukemia virus integration site 1 gene increases ROS production and oxidative stress, which lead to mitochondrial dysfunction, and exacerbate hyperoxia-induced lung injury, and ultimately cause death of lung epithelial cells, contributing to the development of ARDS[11]. Islam et al. observed that, bone marrow mesenchymal stem cells with impaired mitochondria failed to enhance alveolar epithelial cell ATP levels through mitochondrial transfer under lipopolysaccharide stimulation, which significantly decreased the alveolar surfactant and worsened ARDS-related pulmonary edema[12]. Furthermore, Dutra Silva et al. demonstrated the essential role of mitochondria in maintaining the alveolar-capillary endothelial barrier[13]. Harijith et al. reported that hyperoxia upregulates the expression of NADPH oxidase 4, causing mitochondrial dysfunction, triggering the death of type II alveolar epithelial cells, and worsening lung injury in ARDS[14]. Although numerous studies have demonstrated a strong correlation between mitochondrial dysfunction and ARDS, the specific mechanisms of the activation of MRGs and of their contribution to ARDS development have not been explained and need to be further investigated.

Given the crucial role of mitochondrial dysfunction in ARDS, precise identification of cell subsets regulated by MRGs requires research at the single-cell resolution. Unlike traditional transcriptome sequencing, single-cell RNA sequencing (scRNA-Seq) quantifies gene expression at the single-cell level, allowing for simultaneous exploration of transcription in multiple-cell types in tissues and organs[15]. In recent years, scRNA-Seq has improved significantly in sensitivity, accuracy, and efficiency[16]. Increasingly advanced single-cell techniques have also emerged as tools for deciphering the complexity of the pathological mechanisms in various diseases[17]. The integration of machine learning and bioinformatics enables rapid analysis of the relevant transcriptomic and single-cell sequencing data of patients with ARDS, as well as identification of MRG-related biomarkers in ARDS. Through an in-depth analysis of the functions and potential molecular mechanisms of these biomarkers, this study offers a theoretical foundation for improving the diagnosis and treatment of ARDS.

Cell name	Marker gene
Mono	LYZ, CD14, FCGR3A
T	CD3D, CD3E, CD3G
B	CD19, CD79A, CD79B, MZB1
NK	NKG7
NKT	CD3D, CD3E, CD3G, NKG7
Mk	PPBP, PF4

Table 1. Marker genes list.

Materials and methods

Data source

ARDS-related datasets were acquired from the Gene Expression Omnibus (GEO) database (https://www.ncbi.nlm.nih.gov/geo/). The training set GSE32707 (GPL0558) consisted of whole blood samples for 58 sepsis and 31 ARDS (Samples were obtained from Brigham and Women's Hospital, Boston, Massachusetts, USA, collected primarily on October 9, 2011, last updated on July 11, 2012, with some samples updated on 10/7/2020). The validation set GSE66890 (GPL6244) comprised of 28 whole blood samples for sepsis-non-ARDS and 29 whole blood samples for sepsis-ARDS (The samples were obtained from Gladstone Institutes, San Francisco, CA, USA, covering men and women of different ages (e.g., 39, 41, and 66 years old), with disease diagnosis based on the Berlin definition of sepsis with ARDS, and with a sample submission date of 3/13/2015). The single-cell dataset GSE151263 (GPL20301) had 4 peripheral blood mononuclear cell (PBMC) from sepsis-non-ARDS and 3 PBMC samples from sepsis-ARDS. The training, validation and single-cell datasets contain 31,324, 21,131 and 16,788 genes, respectively. There were 11,883 overlapping genes between the three. In addition, the datasets GSE69063 (including 33 healthy samples and 57 sepsis samples) and GSE76293 (including 12 healthy samples and 12 ARDS samples) were selected, totaling 114 samples. After combining these samples, the Combat function in the 'sva' package (version 3.50.0) was used to remove the batch effect and analyze the expression levels of biomarkers. Moreover, 2,030 mitochondria-related genes (MRGs) were taken from MitoCarta 3.0 (https://www.broadinstitute.org/mitocarta/mitocarta30-inventory-mammalian-mitochondrial-proteins-and-pathways) database and the gene set enrichment analysis (GSEA) database (http://www.gsea-msigdb.org/). Approval for this study was obtained from the Ethics Committee of the Second Affiliated Hospital of Guangxi Medical University, No: 2024-KY (0512). All patients and healthy individuals have signed the informed consent form. Research involving human research participants have been performed in accordance with the Declaration of Helsinki.

Differential expression analysis

To get the differentially expressed genes (DEGs) in sepsis-non-ARDS and sepsis-ARDS patients, this study screened the DEGs in the training set data using the R package 'limma' version 3.52.4[18] with adj p value < 0.05 (Correction was carried out using the Benjamini-Hochberg method) and $|\log_2\text{Fold Change (FC)}| > 0.5$. To further obtain the mitochondria-related DEGs, an intersection of the DEGs with MRGs was taken to yield the MRGs-DEGs. To explore the biological functions of the above MRGs-DEGs in the pathogenesis of sepsis-ARDS, Gene Ontology (GO) and Kyoto Encyclopedia of Genes and Genomes (KEGG) for MRGs-DEGs were performed using R package 'clusterProfiler' version 3.18.1[19] with $p < 0.05$.

Identification of candidate key cell types by single-cell data analysis

Based on the single cell dataset, the data was filtered using the NormalizeData function in the R package 'Seurat' version 5.0.1[20]. The percentage of gene count, cell count, and mitochondrial count were calculated. First, cells with fewer than 200 genes and genes expressed in fewer than 3 cells were filtered out. Then, cells with fewer than 200 or more than 3000 expressed genes were removed, along with genes whose expression counts were below 500 or above 10,000. Additionally, the mitochondrial percentage was restricted to less than 10%. The current quality control standard was chosen because a high or low gene expression count indicates poor cell quality and needs to be removed; a high gene count indicates overexpression of genes, which may introduce large errors and needs to be removed[21,22]; and the mitochondrial ratio reflects the degree of damage to the cell, with the more severe the damage, the higher the ratio. In order to reduce the computational effort, after normalizing the data, the 2000 highly variable genes with the highest coefficient of variation between cells were extracted using the variance stabilizing transformation (vst) method. Principal component analysis (PCA) was performed on the various samples in the single-cell dataset. On the one hand, the percentage of standard deviation for each principal component (PC) was ranked and plotted as a PCA inflection point plot. On the other hand, the JackStraw Plot function was applied to compare the distribution of p value for each PC, where notable PCs would have a small p value. After the completion of PCA dimensionality reduction, unsupervised cluster analysis (resolution = 0.4) of the cells was done using the FindNeighbors and FindClusters functions, and the results were visualized with UMAP. Based on the cell clustering results, the marker genes (Table 1) were obtained from reference[23] to annotate the cell clusters as cell types. To capture the mitochondria-related key cell clusters from sepsis-ARDS patients, an AddModuleScore analysis based on the training set of MRGs-DEGs was performed. The AddModuleScore scores of each cell type in every group, such as sepsis-non-ARDS and sepsis-ARDS patients, were calculated based on the gene set and compared between the groups, and the cell types with $p < 0.05$ were finally selected as the candidate key cell types for this study.

Screening for biomarkers

In order to explore feature genes, most minor absolute shrinkage and selection operator (LASSO) logistic regression analysis (5-fold cross validation) was performed for MRGs-DEGs in all samples of the training set using 'glmnet' package version 4.0–2[24], setting the parameter family to binomial (alpha = 1, type.measure = "default"). After running the cv.glmnet function, cross-validation errors were obtained for different lambda values. By selecting the lambda value that minimized the cross-validation error, the model constructed was the optimal one. To further assess and validate the expression trend of these genes in two groups of sepsis-non-ARDS and sepsis-ARDS patients, the expression levels of feature genes were analyzed in both groups of training and validation sets using the Wilcoxon test, respectively. Feature genes with consistent and significant expression trends in the two datasets were defined as biomarkers ($p < 0.05$). To further verify the expression of biomarkers, the datasets GSE69063 and GSE76293 were selected. After removing the batch effect, the Wilcoxon test ($p < 0.05$) was used to compare the expression differences of biomarkers in the healthy group, the sepsis-non-ARDS group and the sepsis-ARDS group.

Artificial neural network (ANN) model

The initial step involved data preprocessing, where the min-max normalization method within the range of [0, 1] was selected. Before the computation, the maximum and minimum data values were normalized, and a single hidden layer with 10 neurons was set (Logistic activation function). During the training process, the gradient propagation of the single hidden layer was relatively stable, with fewer issues of vanishing or exploding gradients. Additionally, a single hidden layer neural network with enough neurons was able to approximate any continuous function. In the training set, the ANN network was constructed based on the biomarkers using the backpropagation method by R package 'neural net' version 1.44.2 (https://CRAN.R-project.org/package=neuralnet), and the weights of the biomarkers were then calculated. Performance evaluation of the ANN model was conducted by generating receiver operating characteristic (ROC) curves for both the training and validation sets.

Function analyses

In the training set, for the purpose of understanding the biological functions of biomarkers in disease development, the Spearman correlation coefficients between each biomarker and all other genes were calculated separately. Then, all the genes were sorted according to the correlation coefficients in ascending order to obtain the list of related genes corresponding to each biomarker. Then we used the 'clusterProfiler' package to perform GSEA to explore the potential functions of the biomarkers based on 'c2.cp.kegg.v2023.1.Hs.entrez.gmt' from MSigDB database as reference gene set. Pathways with enrichment results of $p < 0.05$ and FDR < 0.05 were deemed significant. The top 5 enriched pathways were selected for presentation in order of significance.

Gene set variation analysis (GSVA) was mainly adopted to assess metabolic pathways that were enriched in various samples. Expression matrices of gene sets within 'c2.cp.kegg.v2023.1.Hs.symbols.gmt' from the MSigDB database were calculated according to the biomarkers using the 'GSVA' package version 1.44.5[25]. The expression matrices of various gene sets in the samples were analyzed based on two distinct groups, revealing each group's up- and down-regulation patterns.

To find other genes associated with biomarker function, GeneMANIA (http://www.genemania.org/) was deployed to predict genes linked to biomarker function. It predicted relevant gene interactions by integrating multiple data sources, such as gene co-expression, protein-protein interactions, genetic interactions, pathways, and physical interactions. By entering the gene and species in the top left corner of the database website, the corresponding gene-gene interaction (GGI) network was able to obtain.

Immune infiltration analysis

To further investigate immune cell infiltration between sepsis-non-ARDS and sepsis-ARDS groups, the CIBERSORT algorithm version 6.7-0 was utilized to calculate the level of infiltration of 22 immune cells in both groups[26]. In the total samples of the training set. The difference in immune infiltrating cells between the two groups was then compared by the Wilcoxon test and differential immune cells were obtained ($p < 0.05$; Bonferroni correction was adopted ($\alpha = 0.05/22 \approx 0.0023$)).

Molecular regulatory networks

To inquire whether non-coding RNAs regulated biomarkers, we utilized the miRDB database (https://mirdb.org/) and Targetscan database (https://www.targetscan.org/) to identify miRNAs that could potentially serve as biomarkers (predicted cutoff = 500000). Subsequently, the starBase database (http://starbase.sysu.edu.cn/index.php) was employed to predict target lncRNAs and target circRNAs of miRNAs, and finally lncRNA (circRNA) -miRNA-biomarker regulatory network was created. Meanwhile, the ChEA3 database (https://amp.pharm.mssm.edu/ChEA3) was used to predict transcription factors (TFs) for biomarkers with scores > 1000, leading to the establishment of TF-biomarker network. In addition, to explore potential drugs for the treatment of ARDS, potential drugs targeting biomarkers were searched based on the STITCH database (http://stitch.embl.de/, p less than 0.05 was considered statistically significant), and the biomarker-drug network was visualized through Cytoscape software.

Acquisition of key cell types

Key cell types for sepsis-ARDS were screened by further analyzing the expression of biomarkers in different cell types of the single-cell dataset. Wilcoxon test ($p < 0.05$) was first run for the expression of biomarkers in different cell types, obtaining a remarkable difference in biomarker expression between two groups in the training set to obtain cell types with significant differences in biomarker expression. Cell types with an average number of cells greater than 100 per sample were finally selected as key cell types.

Secondary cluster analysis of key cell types

To further explore the heterogeneity of the critical cell clusters, the functional cell clusters were further analyzed by UMAP clustering re-clustering to obtain their cellular subtypes using the FindNeighbors and FindClusters functions of R package 'Seurat'. In addition, the expression of biomarkers in key cell subtypes was analyzed by Wilcoxon test ($p < 0.05$).

Cell communication analysis

The proportional and numerical distribution of key cell subtypes and other different cell types in sepsis-non-ARDS and sepsis-ARDS groups was first analyzed and demonstrated. Then, communication analysis between key cell subtypes and other cell types was performed with 'CellChat' to calculate aggregated cell-cell communication networks and visualize signals from each cell cluster.

Cell cycle analysis

The cell cycle had wide-ranging effects on cell physiology, regulating differentiation and the expression of gene profiles, and consisted mainly of G1 (pre-DNA synthesis), S (DNA synthesis), G2 (post-DNA synthesis), and M (cytokinesis). In order to deeply investigate and understand how cells regulate their life cycle during different biological processes, with the scRNA-seq dataset, the cycle scores of the S phase and G2M phase of each cell subtype were analyzed using CellCycleScoring based on the expression of cell cycle-related genes in cell subtypes.

Quantitative reverse transcription polymerase chain reaction (qRT-PCR)

Total RNA was isolated from lung tissues or cells using Trizol reagent and chloroform from peripheral blood samples of healthy people and sepsis patients. Reverse transcription and qRT-PCR were detected using the GenStar kit (Kangrunchengye Biotechnology Co., Ltd.; Beijing, China). β-Actin was designated as the internal reference for normalization. The primer sequence is shown in Table 2.

Statistical analysis

Statistical analyses were performed using R software (v 4.2.2). GraphPad Prism 9 and SPSS 23.0 software were utilized for statistical analyses and chart generation. Data following a normal distribution were presented as mean ± standard deviation (SD), and comparisons between the two groups were carried out using the independent sample t-test. A significance level of $p < 0.05$ was considered statistically significant.

Results

A sum of 20 MRGs-DEGs were identified and mainly enriched to mitochondrion related pathways

In the analysis, 343 differentially expressed genes (DEGs) were identified between the sepsis-non-ARDS and sepsis-ARDS groups. Among these, 41 genes were upregulated, while 302 genes were down-regulated in sepsis-ARDS group (Fig. 1A-B). Then 20 MRGs-DEGs were generated by intersecting 343 DEGs with 2,030 MRGs, which were FYN, ALAS2, SGK1, GZMB, RPS27A, MAOA, NDUFAB1, ARL6IP5, TOMM7, HSP90AA1, YWHAB, ARGLU1, RGS2, HSPD1, COX7C, LDHB, SLC2A1, NRGN, IFI27 and C2orf69 (Fig. 1C). Enrichment analysis revealed that MRGs-DEGs enriched 1,084 GO pathways, among which there were 785 biological processes (BP), including 'regulation of intracellular protein transport' (GO: 0033157), 'protein targeting' (GO: 0006605), 'regulation of intracellular transport' (GO: 0032386), 'establishment of protein localization to mitochondrion' (GO: 0072655), 'protein localization to mitochondrion' (GO: 0070585), etc. There were 122 items of cellular component (CC), including 'mitochondrial inner membrane' (GO: 0005743), 'mitochondrial outer membrane' (GO: 0005741), 'organelle outer membrane' (GO: 0031968), 'outer membrane' (GO: 0019867), 'mitochondrial matrix' (GO: 0005759), etc. There were 117 items for molecular function (MF), including 'ubiquitin protein ligase binding' (GO: 0031625), 'ubiquitin-like protein ligase binding' (GO: 0044389), 'disordered domain specific binding' (GO: 0097718), 'ATP-dependent protein folding chaperone' (GO: 0140662), 'tau protein binding' (GO:0048156) and so on (Fig. 1D). By KEGG enrichment analysis, MRGs-DEGs were mainly enriched to 'glycine, serine and threonine metabolism', 'HIF-1 signaling pathway', 'PI3K-Akt signaling pathway' and other pathways (Fig. 1E).

Altogether 6 cell types were annotated in single cell dataset

The single-cell dataset comprised 24,796 cells and 16,788 genes prior to data filtering, with 24,102 cells and 16,788 genes remaining following filtering (Fig. 2A). 2000 highly variable genes were then selected for further analysis (Fig. 2B). Also, PCA indicated that the cells from the different samples in the control and disease groups were mixed together in a more concentrated distribution and could therefore be analyzed normally (Fig. 2C). Through the PCA inflection plot, the trend of p value was larger before 30 PCs and smaller after 30 PCs, so dims = 30 (the top 30 PCs) and resolution = 0.4 were chosen for subsequent analyses (Fig. 2D). After completing PCA, all cells were divided into 19 clusters in UMAP (Fig. 2E). These cell clusters were annotated to altogether 6 cell types, namely monocytes (Mono), T cells, B cells, NK cells, NKT cells and Mk cells (Fig. 2F). Meanwhile, expression of marker genes in every cell type was shown in Fig. 2G. The results of AddModuleScore score difference analysis showed that AddModuleScore scores of monocytes, T cells, NKT cells, NK cells, and Mk cells were markedly different between two groups ($p < 0.05$). Therefore, these 5 types of cells were screened as the candidate key cell types (Fig. 2H).

Gene	Species	Primer sequence (5'–3')
IFI27-F	Homo	TGTGATTGGAGGAGTTGTGGC
IFI27-R	Homo	CAATCCGGAGAGTCCAGTTGC
SLC2A1-F	Homo	GCTTCCAGTATGTGGAGCAACT
SLC2A1-R	Homo	GTCTTGTCACTTTGGCTGGCT
β-Actin-F	Homo	AGATCAAGATCATTGCTCCTCCTG
β-Actin-R	Homo	AGTCATAGTCCGCCTAGAAGCAT

Table 2. Primer sequence.

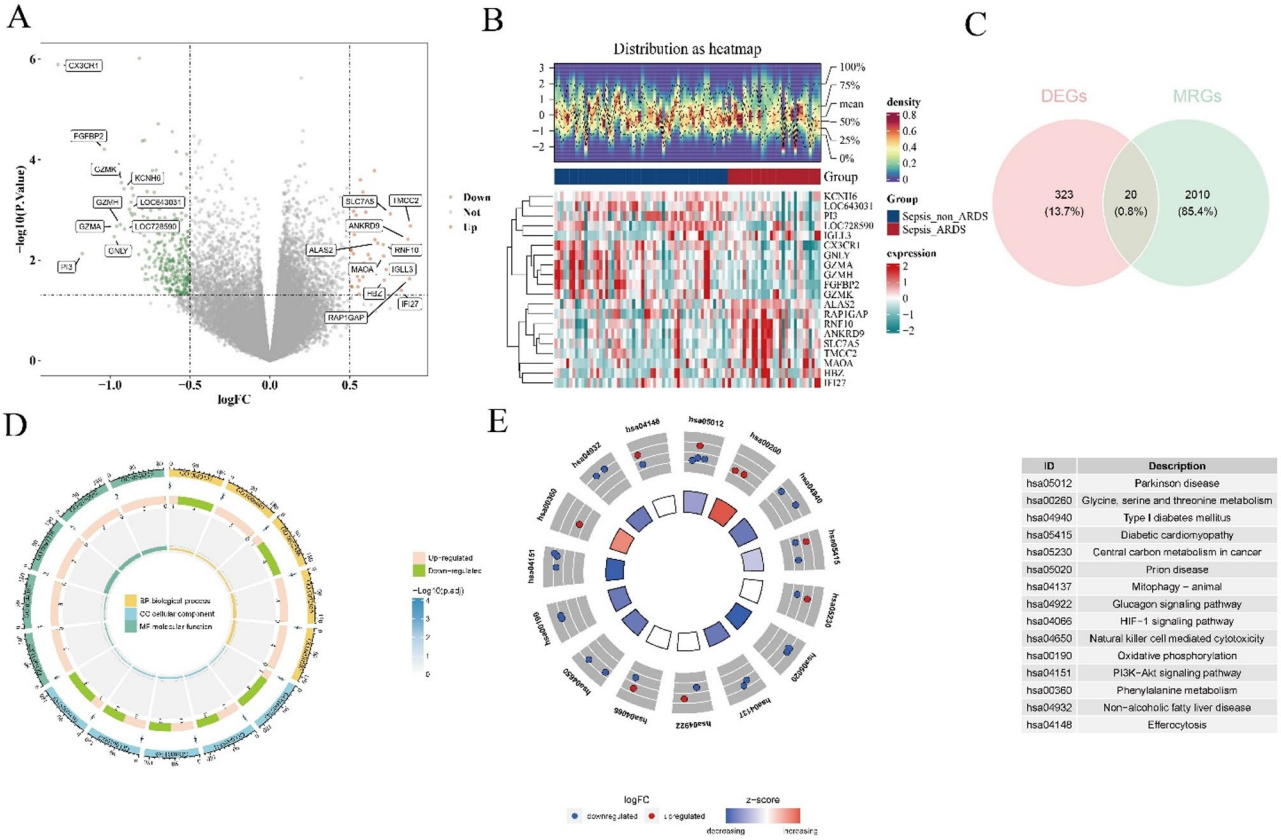

Fig. 1. Identification of candidate MRGs-DEGs. **A** Volcano map of MRGs-DEGs between sepsis-non-ARDS group and sepsis-ARDS group in GSE32707 dataset. **B** Heatmap of DEGs from GSE32707 dataset. **C** Venn plot of genes of MRGs-DEGs and DEGs. **D** GO enrichment analysis of DEGs. **E** KEGG pathway enrichment analysis of DEGs.

SLC2A1 and IFI27 were defined as biomarkers

According to the LASSO model, a total of 9 feature genes were screened out when log (lambda. min) = −3.808265, namely ALAS2, SGK1, GZMB, MAOA, HSP90AA1, COX7C, SLC2A1, NRGN and IFI27 (Fig. 3A-B). SLC2A1 and IFI27 were expressed differently between two groups of patients with sepsis-non-ARDS and sepsis-ARDS in the training and validation sets. Notably, both genes were upregulated in the sepsis-ARDS group compared to the sepsis-non-ARDS group. Therefore, SLC2A1 and IFI27 were defined as biomarkers in this study (Fig. 3C-D). Next, the datasets GSE69063 and GSE76293 were selected. After removing the batch effect (**Supplementary Fig. 1A-B**), the expression differences of IFI27 and SLC2A1 in the healthy group, the sepsis-non-ARDS group and the sepsine-ARDS group were compared. The results indicated that there were significant differences between IFI27 and SLC2A1 among these three groups (**Supplementary Fig. 1C**).

ANN network had a better differentiation effect

The ANN network was structured upon two biomarkers (SLC2A1 and IFI27) to identify weights of biomarkers (Fig. 4A). The ROC curves displayed area under the curve (AUC) values of 0.7386 and 0.7020 for the two datasets, indicating that the ANN network constructed in the two datasets had a good differentiation effect between sepsis-non-ARDS and sepsis-ARDS groups (Fig. 4B-C).

Potential functions of biomarkers

GSEA results showed that the pathways significantly enriched under the IFI27 subgroup were 'ribosome', 'proteasome', 'Parkinsons disease', 'oxidative phosphorylation' and 'spliceosome', and these pathways were presumed to be notably positively correlated with IFI27 (Fig. 5A). Pathways significantly enriched under the SLC2A1 subgroup were 'ribosome', 'Parkinsons disease', 'Huntington's disease', 'chronic myeloid leukemia' and 'olfactory transduction', of which only 'olfactory transduction' was presumed to be markedly negatively correlated with SLC2A1 and the rest were notably positively correlated (Fig. 5B). Additionally, up- and down-regulation trends of gene sets in sepsis-non-ARDS and sepsis-ARDS groups were obtained by GSVA (Fig. 5C). The gene sets that were upregulated relative to the sepsis-non-ARDS group were 'HEDGEHOG signaling pathway', 'glycine-serine and threonine metabolism', 'taste transduction', 'basal cell carcinoma', 'tyrosine metabolism'. The set of genes that were downregulated relative to the sepsis-non-ARDS group was 'basal transcription factors', 'cytokine-cytokine receptor interaction', 'T-cell receptor signaling pathway', 'JAK-STAT signaling pathway',

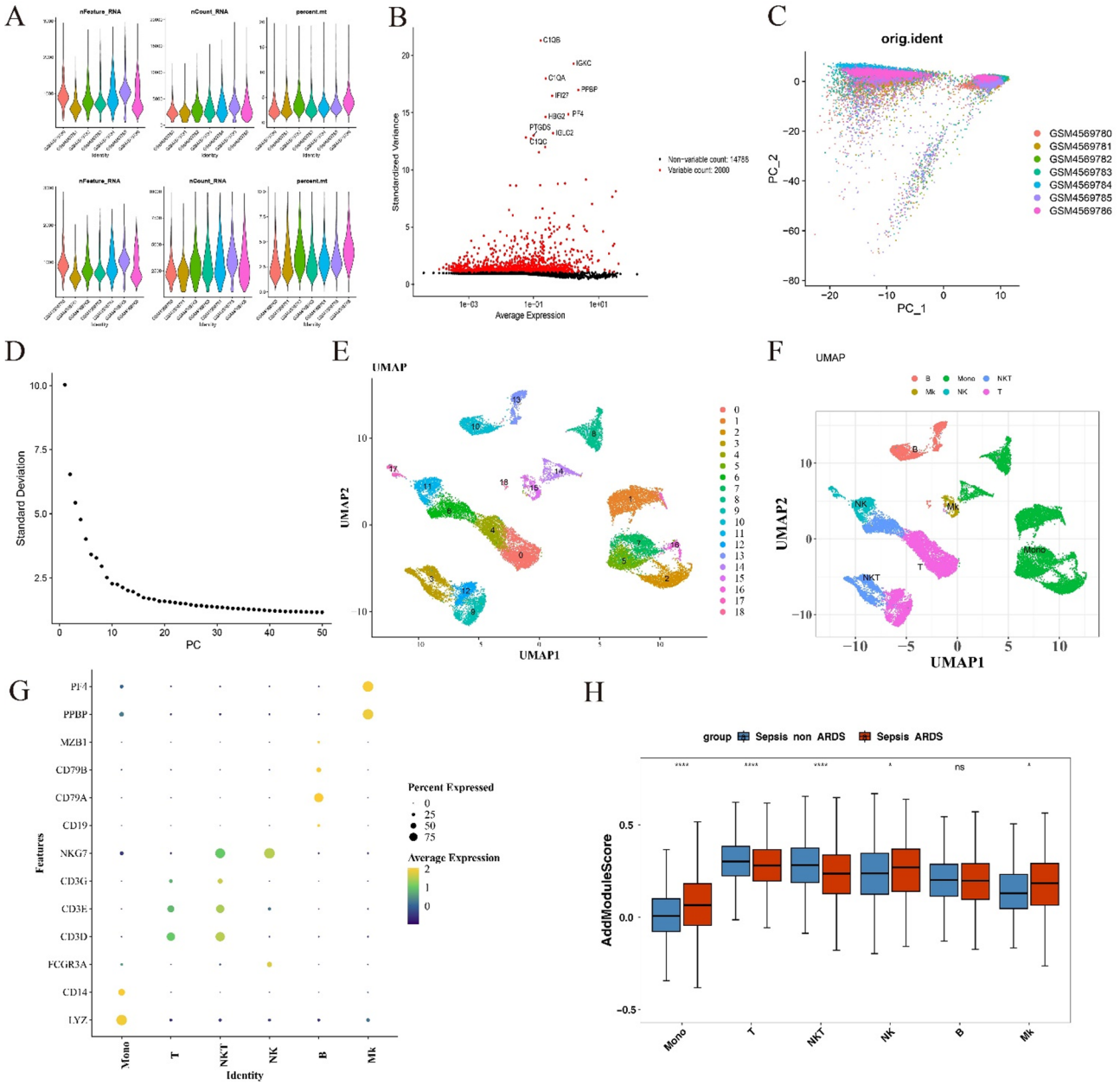

Fig. 2. **A-B** Comparison of results before and after quality control. **C** Screening of highly variable genes. **D** Cell distribution of PCA sample. **E** Cell UMAP cluster map. **F** Cell annotation UMAP. **G** The expression levels of different cell clusters were visualized according to their markers. **H** The Add Module Score of different cell types in sepsis-non-ARDS and sepsis-ARDS patients were compared. Ns $p>0.05$, *$p<0.05$, ****$p<0.0001$.

'tryptophan metabolism' and 'natural killer cell-mediated cytotoxicity'. Furthermore, we demonstrated the interactions between 2 biomarkers and 20 other predicted genes through the GGI network, which were STOM, IFI6, ASPSCR1, IFI27L1, IFI27L2, NR4A1, IRF9, STXBP3, HK2, HK1, HK3, STAT2, HDAC7, STAT1, DMTN, ISG15, SLC2A4, IFITM1, MX1 and HIF1A (Fig. 5D).

The Naive B cells, and Naive CD4 + T cells were differential immune cells

Of the total 89 samples in the training set, 85 samples were included for immune cell infiltration analysis after excluding samples with p values less than 0.05. The percentage of 22 immune cell infiltrates in these samples were demonstrated in Fig. 6A. Between sepsis-non-ARDS and sepsis-ARDS groups, naive B cells, and naive CD4 + T cells were significant differences, with naive B cells and naive CD4 + T cells upregulated and resting NK cells downregulated relative to the sepsis-non-ARDS group (Fig. 6B).

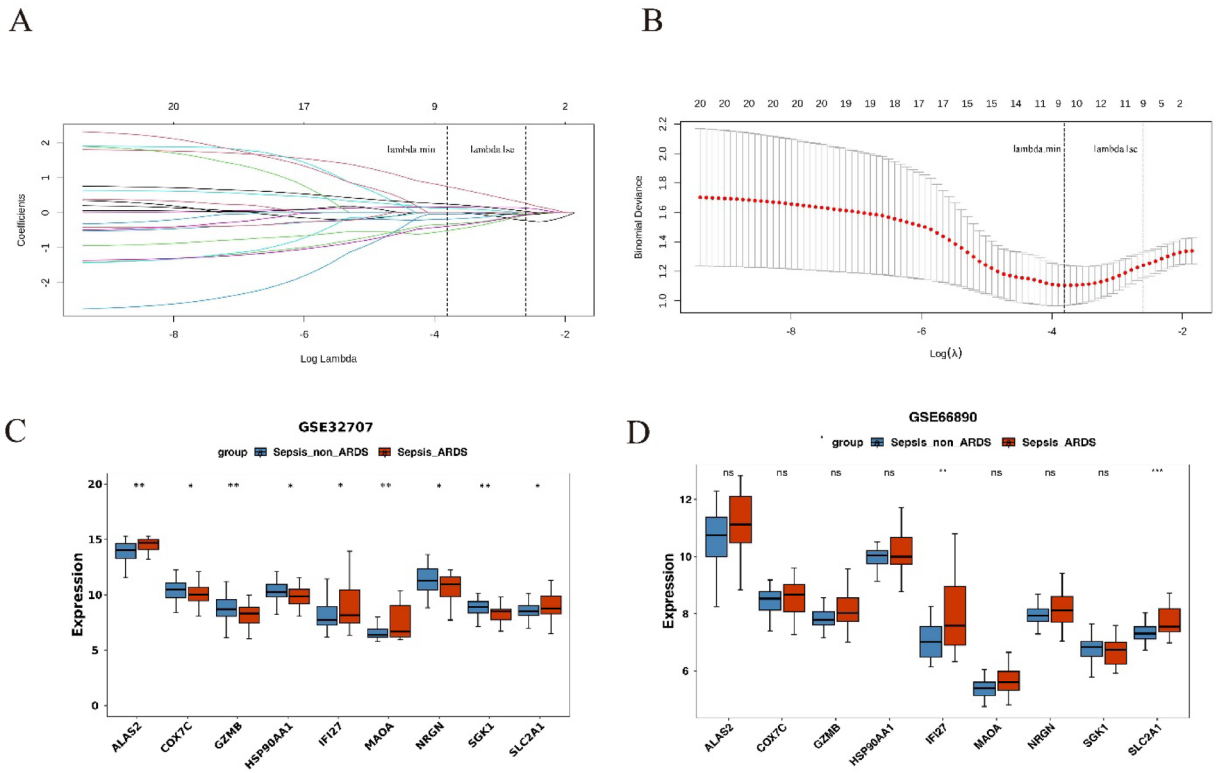

Fig. 3. Identification of characteristic MRGs-DEGs. **A** Gene coefficient pattern of Lasso regression analysis for 20 MRGs-DEGs. **B** Error graphs for cross validation of Lasso regression analysis for 20 MRGs-DEGs. **C**: training set; **D**: verification set. Expression levels of characteristic genes in patients with sepsis-non-ARDS and sepsis-ARDS. Ns $p>0.05$, *$p<0.05$, ** $p<0.01$, *** $p<0.001$.

The lncRNA(circRNA)-miRNA-biomarker, TF-biomarker and biomarker-drug networks were developed for biomarkers

The lncRNA (circRNA)-miRNA-biomarker regulatory network consisted of 56 nodes and 125 edges, with 4 miRNAs, 30 circRNAs, 21 lncRNAs and 2 biomarkers (Fig. 6C). The TF-mRNA network demonstrated 14 TFs for 2 biomarkers, and IFI27 was predicted to have only one TF: HDX (Fig. 6D). Also, biomarker-drug network had 12 nodes and 22 edges, and the predicted drugs included pentobarbital, dehydroascorbic, and phloretin, which might act through the target gene (Fig. 6E).

Mono was the key cell type and subdivided into CD14 and CD16 subtypes

As a further step to screen the key cell clusters for sepsis-ARDS, we compared the expression of the two biomarkers in different cell types, and the results presented that both IFI27 and SLC2A1 were markedly different in Mono, B and Mk cells (Fig. 7A-B). Combining the 5 candidate key cell types obtained previously, and since the number of Mk cells was only 507 in the 7 samples, with an average of less than 100 cells per sample, which was insufficient to support subsequent in-depth single-cell analyses, we finally defined Mono as key cell type. To further explore the critical cell types, a secondary clustering analysis of Mono was performed, which showed that monocytes could be subdivided into two cell subtypes CD14 (CD14+, LYZ+) and CD16 (FCGR3A+, LYZ+) (Fig. 7C-D). Next, the expression of IFI27 and SLC2A1 in monocyte subtypes CD14 and CD16 was analyzed. The results showed that there were significant differences in these biomarkers in both CD14 and CD16 subtypes (**Supplementary Fig. 2**).

Cellular communication and cell cycle between key cell subtypes

Firstly, the proportions and number distribution of Mono cell subtypes with other cell types in the sepsis-non-ARDS and sepsis-ARDS groups were demonstrated, and the proportions of almost all cell types differed in the two groups. In particular, the proportion of CD16 Mono, B, and T infiltrate proportion was markedly higher in sepsis-ARDS group than in the sepsis-non-ARDS group. In contrast, the proportions of Mk, NK, and NKT cells were notably lower than in the sepsis-non-ARDS group (Fig. 7E). These changes suggested that sepsis-ARDS group might alter interactions between various cell types. Further communication analyses showed that the sepsis-ARDS group had enhanced CD14 monocytes and B cells. The interaction between CD14 monocytes and CD16 monocytes was attenuated compared with the sepsis-non-ARDS group (Fig. 7F). Moreover, cycle score analyses showed that CD16 had a higher percentage and score in G2M and S phases and a lower percentage and score in G1 phase, relative to CD14 (Fig. 7G-H).

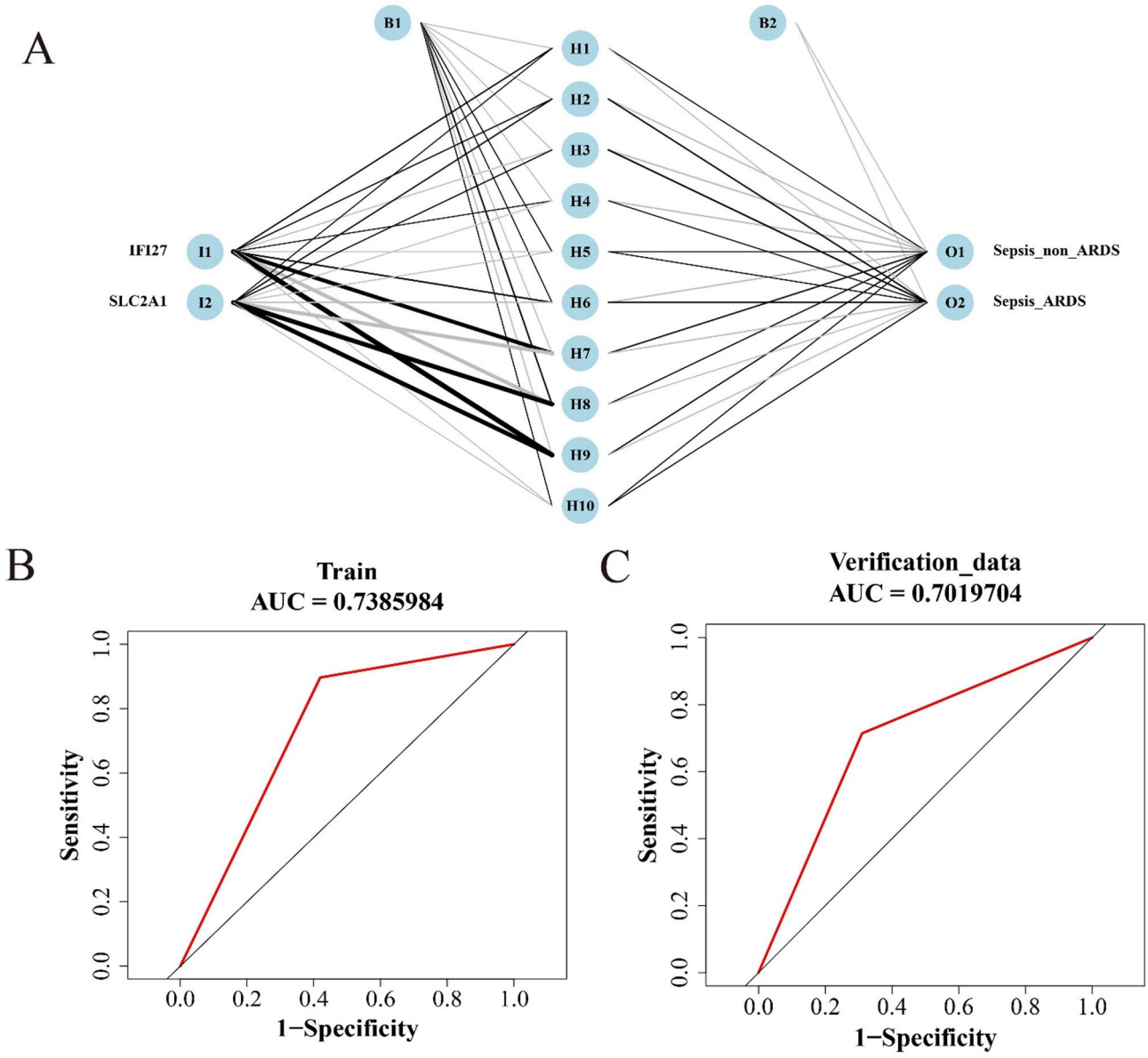

Fig. 4. **A** Artificial neural network model. **B-C** ROC curve evaluates the classification effectiveness of artificial neural network.

Expression difference between IFI27 and SLC2A1 in monocyte types and clinical samples

The expression of IFI27 and SLC2A1 in the identified monocytes was different in CD14 monocytes, and the results were upregulated (Fig. 8A-B). However, differences could not be compared due to the small number of CD16 cells. Peripheral blood samples from sepsis patients were obtained for qRT-PCR detection. Compared with healthy individuals, the mRNA of IFI27 and SLC2A1 was significantly upregulated (Fig. 8C-D).

Discussion

ARDS is defined as a severe respiratory disease marked by bilateral chest imaging opacity and profound hypoxemia due to noncardiogenic pulmonary edema, representing a critical form of respiratory failure. However, its current treatment plan has a poor therapeutic effect, necessitating a more specific treatment. Mitochondrial dysfunction has been identified as a critical factor in the pathogenesis of ARDS, but the patterns of immune infiltration and the interaction between immune regulation and mitochondrial function in ARDS have yet to be fully elucidated. Advances in gene therapy research enable the targeting of mitochondrial dysfunction and oxidative stress, potentially helping inhibit ARDS progression. The identification of mitochondrial-related biomarkers is urgently needed to guide new approaches to the diagnosis and treatment of this disease.

In this study, SLC2A1 and IFI27 were identified as potential mitochondria-related biomarkers for ARDS through a series of bioinformatics analyses, including differential analysis and machine learning. SLC2A1 is an essential glucose transporter involved in energy metabolism. Numerous studies have highlighted abnormal

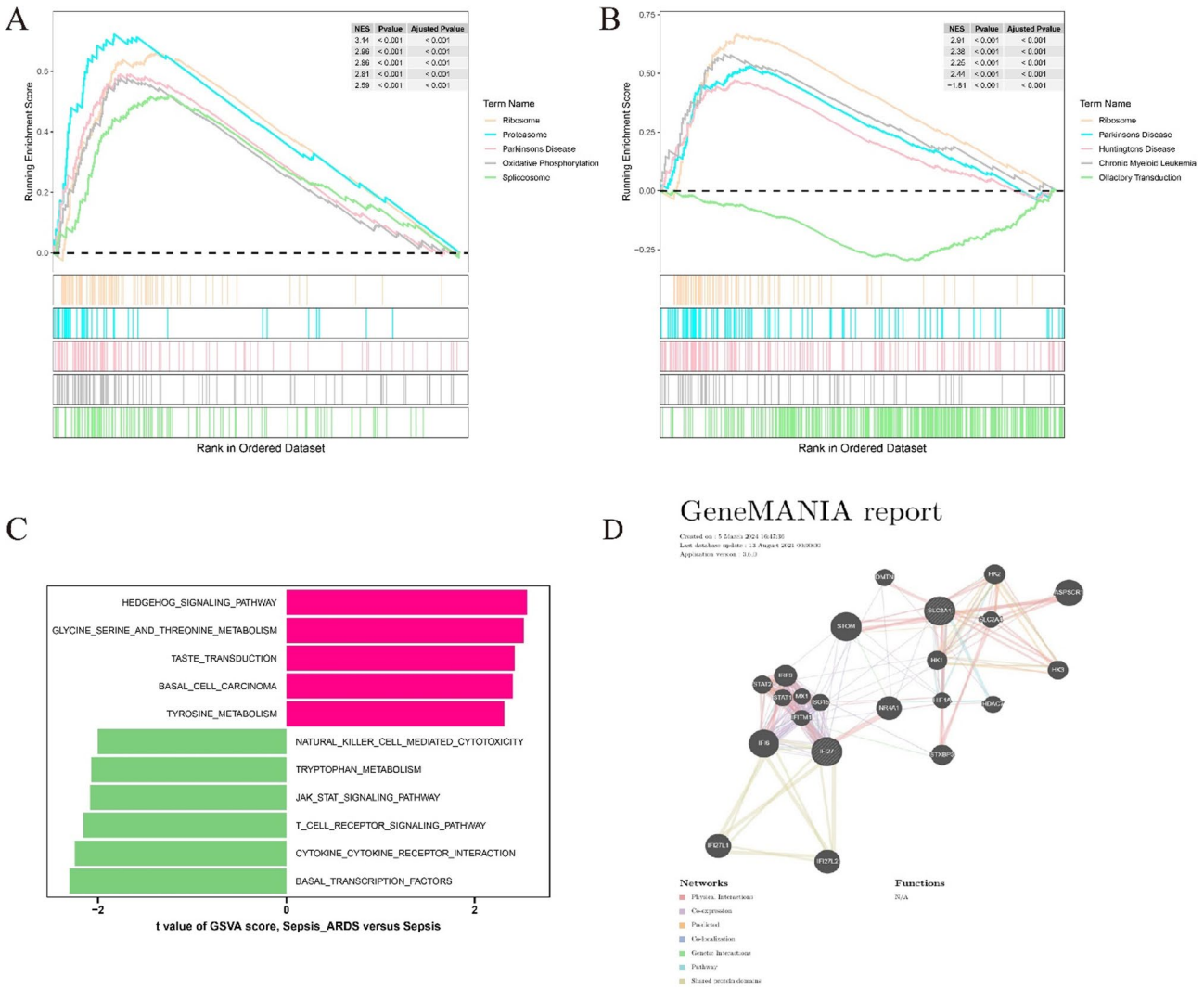

Fig. 5. **A-B** GSEA enrichment analysis of IFI27 and SLC2A1. **C-D** The up-down-regulation trend of IFI27 and SLC2A1 in sepsis-non-ARDS and sepsis-ARDS group was analyzed by GSVA.

expression levels of this gene in various diseases, including colorectal cancer[27], lung adenocarcinoma[28], gastric cancer[29,30], intraductal mucous tumor[31], and hepatocellular carcinoma[32]. For example, Liu et al. found elevated SLC2A1 levels in patients with colorectal cancer, which they associated with immune invasion, m6A modification, and apoptosis, suggesting that SLC2A1 is a potential biomarker for colorectal cancer[27]. Moreover, significant upregulation of SLC2A1 expression levels has been reported in patients with lung squamous cell carcinoma, demonstrating a negative correlation with immune checkpoint molecules[33]. Research has indicated that SLC2A1 overexpression can increase glucose uptake, glucose metabolism, and the levels of pentose phosphate pathway intermediates, and decrease cellular oxygen consumption. These influence glucose metabolism and macrophage metabolic programming, which leads to heightened production inflammation[34]. SLC2A1 mutations lead to glucose transporter type 1 deficiency syndrome and are regarded as rare contributors to pediatric hereditary spastic paraplegia[35]. Posttranslational lipid modifications include palmitoylation, and many soluble and membrane-attached proteins are known to facilitate palmitoylation, which is associated with various diseases, including Huntington's disease and Alzheimer's disease. Among the approximately 400 solute carriers of 66 gene families, the most apparent transporters include SLC2A1, SLC2A4, and SLC6A2[36]. Energy metabolism disorders are also present in sepsis patients. These findings indicated that SLC2A1 may be involved in energy metabolism, oxidative stress, and other related processes and, thus, could be a promising biomarker for disease diagnosis and prognostic assessment. However, the precise diagnostic and prognostic implications of SLC2A1 in sepsis remain unclear. In this research, SLC2A1 was identified as a novel biomarker for sepsis-ARDS, providing potential insights for the diagnosis and management of sepsis and sepsis ARDS.

IFI27 was identified as another biomarker for sepsis-ARDS in this study. Studies have shown that increased expression levels of invasive alveolar macrophage subsets and blood immune cells in COVID-19 patients could be used as biomarkers for mitochondrial immunity to evaluate viral infection severity[37]. Furthermore, dysregulation of IFI27 expression in chronic inflammatory diseases may contribute to the recruitment of inflammatory

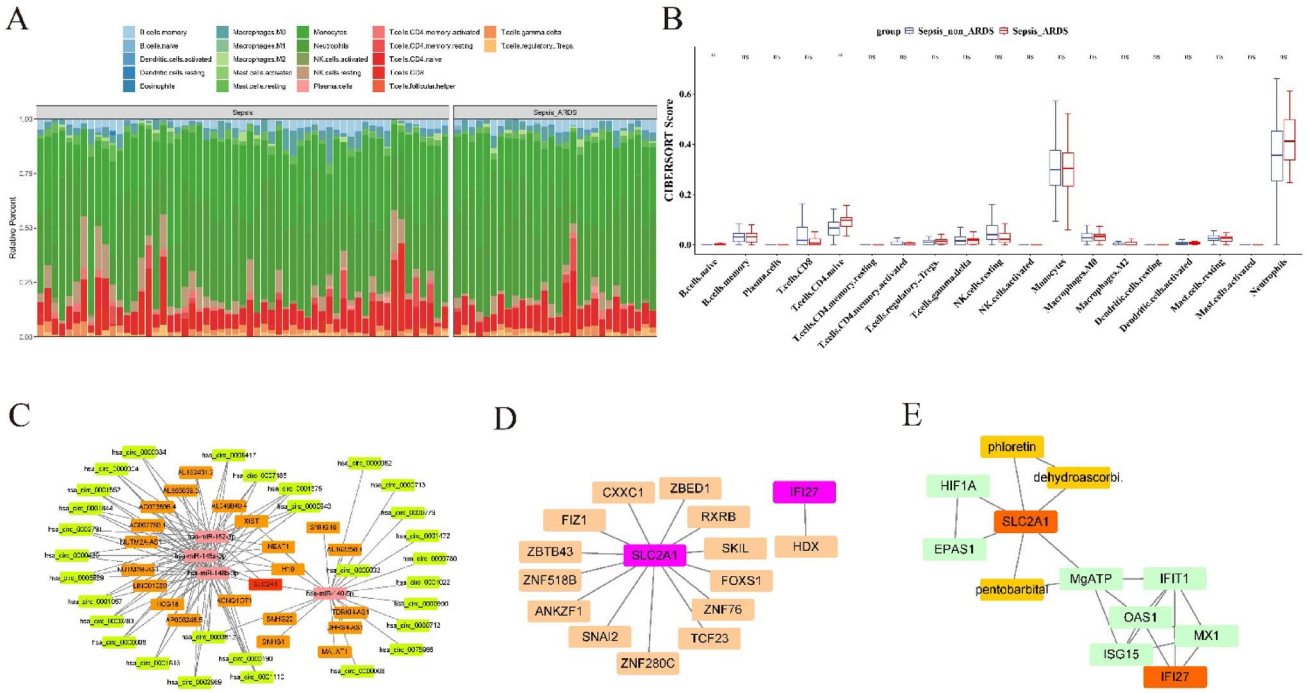

Fig. 6. **A** Immune cell infiltration between sepsis-non-ARDS group and sepsis-ARDS group. **B** Differences of immune cells between sepsis-non-ARDS and sepsis-ARDS group. **C** Non-coding RNA regulatory networks. **D** Differential TFS-biomarker relationship network. **E** Biomarker - drug network diagram.

processes and the destruction of immune balance[38]. Recent studies have shown high IFI27 expression levels in patients with COVID-19-induced ARDS, with the Mono-IFI27 subgroup significantly enriched under the combined influence of immunosuppression and viral infection, potentially impeding immune reconstitution[39]. Xu et al. demonstrated that the model based on IFI27 exhibited promising recognition capabilities for sepsis-non-ARDS and sepsis-ARDS, indicating its potential as a diagnostic feature for the latter[40]. Research has demonstrated that IFI27 is prominently expressed in brown fat, localized explicitly in mitochondria, and can be stimulated by β3-adrenergic activation in adipose tissue[41]. Suppression of IFI27 has been shown to impede the expression of crucial genes involved in genes of physiological energy metabolism in adipocytes, including the tricarboxylic acid cycle and respiratory chain transmission[41]. Furthermore, analysis of transcriptome sequencing and validation of peripheral blood mononuclear cells in individuals with severe hand, foot, and mouth disease (HFMD) due to enterovirus 71 revealed that IFI27 may be an indicator of the HFMD severity[42]. These findings further corroborate the results of the present study. Therefore, actively exploring the link between genes and pathways may lead to promising therapeutic prospects for patients with sepsis.

Additionally, this study identified monocytes as the key cell types, and the secondary cluster analysis revealed that monocytes could be further classified into two subtypes: CD14 and CD16. Previous research has indicated that gene abnormalities mediated by monocytes potentially contribute significantly to the developments and advancement of ARDS[39]. Moreover, the inhibition of monocytes has been shown to mitigate the immunosuppressive effects of sepsis[43]. Even repaired monocytes exhibit low immunogenicity and have demonstrated potential immunomodulatory effects by reducing inflammation in experimental sepsis mouse models[44]. Monocyte clusters in ARDS patients, especially CD16 cells, exhibit various pro-inflammatory characteristics and upregulation of multiple type 1 IFN-induced gene expressions[39]. Furthermore, patients with sepsis often have an increased number of monocytes that express CD16[+ 45], and evidence shows a significant increase in circulating counts of patrolling monocytes for up to 10 days[46]. Furthermore, we performed comprehensive cell communication and cycle analyses on monocytes, offering new insights into ARDS pathogenesis. Emerging evidence indicates that ARDS modulates immune cell dynamics through intercellular communication, with cell cycle regulation appearing intrinsically linked to immune cell proliferation and functional reprogramming, thereby influencing disease progression[47]. Another study indicates that intercellular signaling pathways facilitate the aggregation and activation of immune effector cells through cytokine-mediated interactions and ligand-receptor binding mechanisms. During the pathogenesis of ARDS, the proliferative expansion and functional alterations of immune cells demonstrate significant correlation with cell cycle modulation, suggesting a potential regulatory mechanism that may critically influence disease trajectory and clinical prognosis[48]. The results of the present study revealed differential expression of the biomarkers IFI27 and SLC2A1 in CD14 monocytes during sepsis-non-ARDS and sepsis-ARDS. The mRNA expression levels of IFI27 and SLC2A1 in the peripheral blood of the sepsis patients were upregulated compared with those of the healthy individuals, consistent with the predicted results. These results further underscore the significance of monocytes in the pathogenesis of sepsis and validate the reliability of our findings.

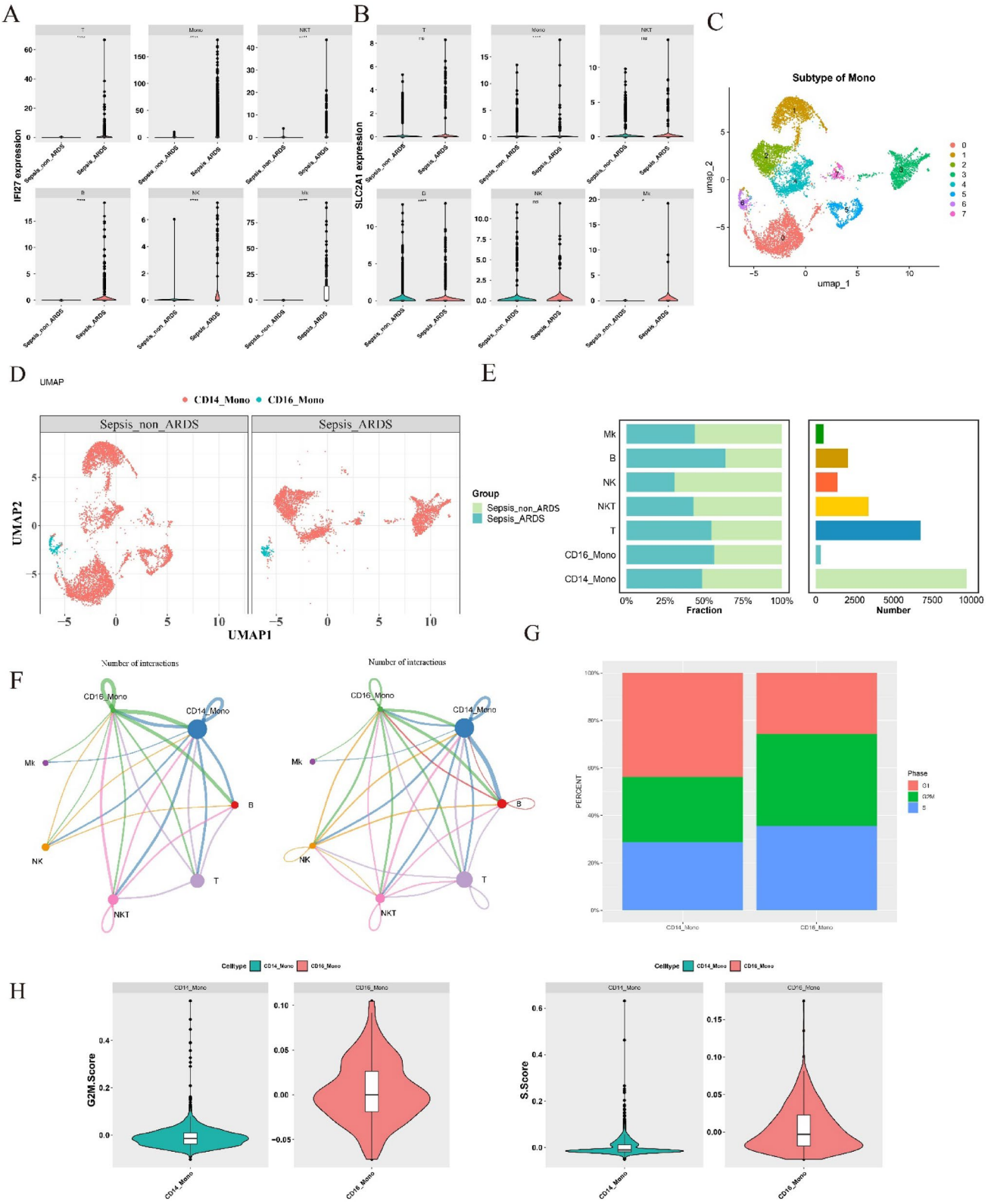

Fig. 7. **A** Expression of IFI27 in different cell clusters. **B** Expression of SLC2A1 in different cell clusters. **C** The key cell cluster Mono was analyzed by UMAP clustering and regrouping. **D** UMAP of Mono cell subpopulation identification. **E** The proportion and number distribution of Mono cell subtypes versus other cell types in sepsis-non-ARDS and sepsis-ARDS groups. **F** Cell-to-cell communication network between Mono cell subtypes and other cell types. **G-H** Cell cycle proportion and score analysis of Mono cell subtypes. Ns $p > 0.05$, $^{*}p<0.05$, $^{****}p<0.0001$.

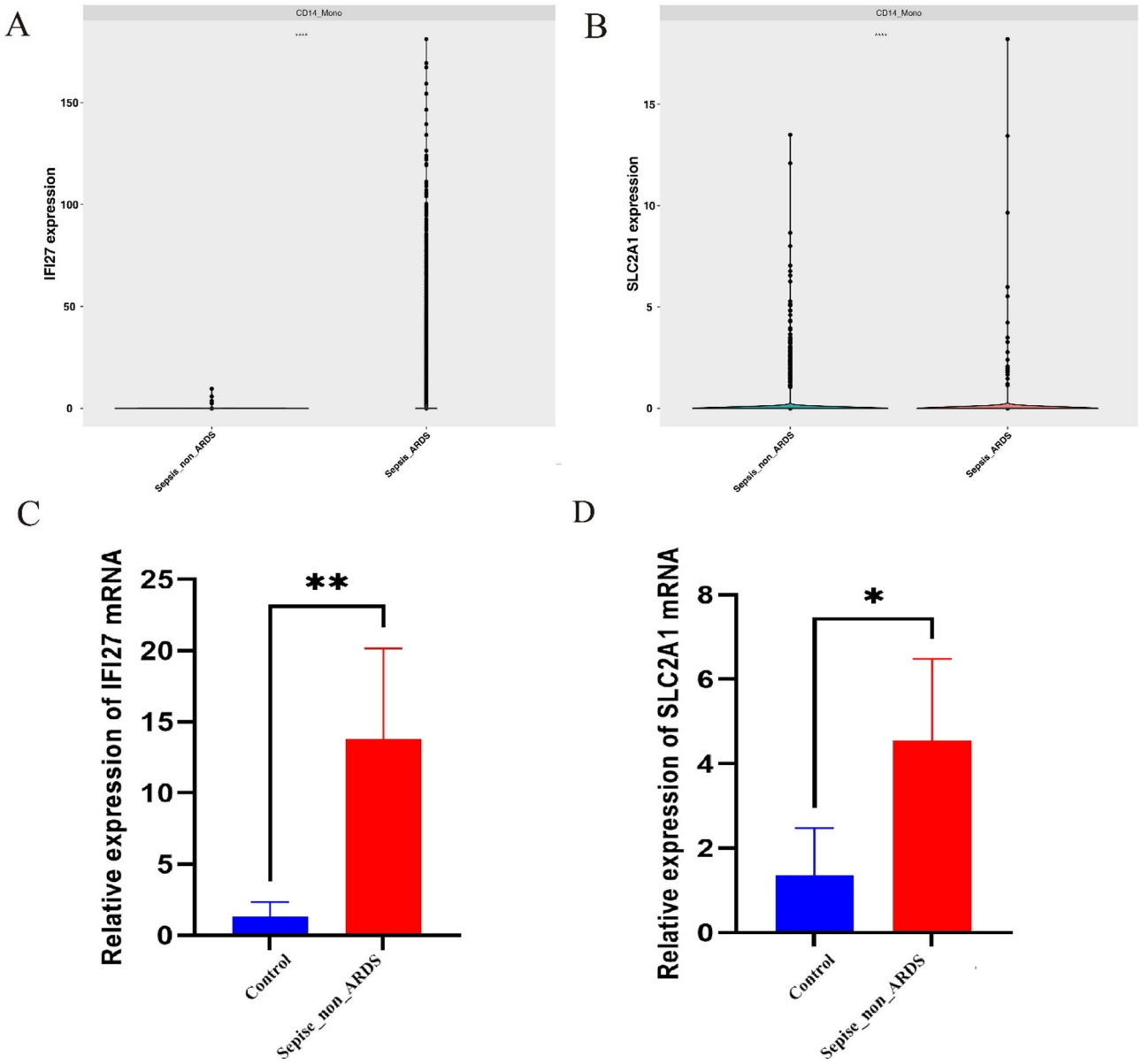

Fig. 8. **A** Expression of IFI27 in CD14 monocytes. **B** Expression of SLC2A1 in CD14 monocytes. **C** The relative expression of IFI27 mRNA in human peripheral blood (Control group: $n = 5$; Sepsis-non-ARDS group: $n = 4$). **D** The relative expression of SLC2A1 mRNA in human peripheral blood (Control group: $n = 5$; Sepsis-non-ARDS group: $n = 4$). $^{*}p<0.05$, $^{**}p<0.01$, $^{****}p<0.0001$.

In this study, four miRNAs targeting SLC2A1—hsa-miR-152-3p, hsa-miR-148a-3p, hsa-miR-148b-3p, and hsa-miR-140-5p—were predicted by constructing ncRNA regulatory networks. Among these, hsa-miR-152-3p has been recognized as associated with diabetic nephropathy in individuals with type 2 diabetes and as closely correlated with plasma osmotic pressure[49]. In patients with Tibetan gastric cancer, the expressions levels of hsa-miR-148a-3p and hsa-miR-148b-3p were downregulated and significantly enriched in pathways related to cancer[50]. The fourth miRNA, hsa-miR-140-5p, is involved in the regulating fat and cholesterol metabolism, correlates significantly with serum marker CK-18, and negatively regulates hepatic low-density lipoprotein receptors in human hepatocytes[51,52]. Recent research has been delved deeper into the role of noncoding RNA in sepsis-non-ARDS and sepsis-ARDS and has yielded promising outcomes. For instance, targeting SLC2A1 with exosome has-miR-1262 in the peripheral blood of patients with sepsis has been found to be capable of suppressing bit glycolysis and inducing apoptosis in human cardiomyocytes[53]. Another study showed that miRNA-22 modulates the proinflammatory response and M1 polarization of macrophages by targeting SLC2A1[54]. Our recent research has shown that miRNA-206-3p plays a role in acute lung injury by targeting specific genes regulating cellular pathways that control pyroptosis and inflammatory responses[55]. In addition, pentobarbital, dehydroascorbic acid, and phloretin have been found to be potentially useful in the treatment of septicemic-induced ARDS. Accumulating evidence demonstrates that GLUT1, encoded by the SLC2A1 gene,

serves crucial roles in erythrocyte metabolism by facilitating cellular uptake of dehydroascorbic acid, thereby ameliorating oxidative damage through antioxidant regeneration mechanisms[56]. Pharmacological studies reveal that phloretin, a specific GLUT1 inhibitor, effectively modulates glucose transport dynamics and influences the odontogenic differentiation potential of human dental pulp stem cells[57]. Notably, despite these mechanistic insights, no systematic investigations have been conducted to explore the therapeutic potential of GLUT1-targeting compounds in ARDS management. The research team intends to further investigate these genes and drugs and to validate them in both in *vivo* and in *vitro* experimental models in the future.

The current research has some limitations. Firstly, the ANN model lacks an independent test set, which is prone to overfitting on the validation set. Therefore, in future studies, an independent test set should be introduced to improve the generalization ability of the model. Secondly, the design differences among the healthy group, the sepsis-non-ARDS group and the sepsis-ARDS group may cause confusion. In the future, it is necessary to refine the groups and ensure the distinction of the characteristics of each group to enhance the accuracy of the results. Furthermore, the sample size is limited and protein validation experiments have not yet been conducted. In the future, the sample size should be expanded and more protein-level validation experiments should be carried out to enhance the credibility of statistical analysis and verify the practical application of biomarkers. Finally, the regulatory mechanism of the TF-mRNA network lacks sufficient experimental verification. Future research will focus on verifying its biological functions. These improvements will provide a more solid foundation for future research, promote the optimization of the model and facilitate its application and promotion in clinical practice.

The strength of this study lies in its utilization of single-cell sequencing data and transcriptomics to identify two crucial mitochondrial genes (SLC2A1 and IFI27) linked to sepsis-non-ARDS and sepsis-ARDS. These genes were identified as biomarkers using the LASSO model. Upregulation of the expression of these genes was notably observed in patients with sepsis. Furthermore, the comparison of their expression levels across different cell types highlighted monocytes as the vital cell type. In this study, only a small sample size was collected to verify the mRNA expressions of IFI27 and SLC2A1 in peripheral blood samples of healthy individuals and patients with sepsis, with no comparison made between patients with sepsis and those with sepsis-ARDS. However, the validation results preliminarily showed that the mRNA levels of IFI27 and SLC2A1 were significantly elevated compared to those in the healthy individuals, indicating the accuracy of single-cell sequencing combined with transcriptomics. Moving forward, we will continue to examine the mechanisms of IFI27 and SLC2A1 that influence the development and the progression of sepsis-non-ARDS and sepsis-ARDS.

Data availability

The datasets analysed during the current study are available in the [Gene Expression Omnibus (GEO) database] repository, [https://www.ncbi.nlm.nih.gov/geo/]https://www.ncbi.nlm.nih.gov/geo/query/acc.cgi? acc=GSE32707, https://www.ncbi.nlm.nih.gov/geo/query/acc.cgi? acc=GSE66890, https://www.ncbi.nlm.nih.gov/geo/query/acc.cgi? acc=GSE151263.

Received: 28 July 2024; Accepted: 24 July 2025
Published online: 02 August 2025

References

1. Bos, L. D. J. & Ware, L. B. Acute respiratory distress syndrome: causes, pathophysiology, and phenotypes . *Lancet.* **400**(10358), 1145–1156 (2022).
2. Bellani, G. et al. Epidemiology, patterns of care, and mortality for patients with acute respiratory distress syndrome in intensive care units in 50 countries. *Jama.* **315**(8), 788–800 (2016).
3. Zhang, S. et al. Breath metabolomics for diagnosis of acute respiratory distress syndrome. *Critical care.* **28**(1), 96 (2024).
4. Confalonieri, M., Salton, F. & Fabiano, F. Acute respiratory distress syndrome. *Eur Respir Rev.* **26**(144), 160116 (2017).
5. Grotberg, J. C., Reynolds, D. & Kraft, B. D. Management of severe acute respiratory distress syndrome: a primer. *Critical care.* **27**(1), 289 (2023).
6. Andrieux, P. et al. Mitochondria as a cellular hub in infection and inflammation. *Int J Mol Sci.* **22**(21), 11338 (2021).
7. Brea-Calvo, G. et al. COQ4 mutations cause a broad spectrum of mitochondrial disorders associated with CoQ10 deficiency. *Am J Hum Genet.* **96**(2), 309–317 (2015).
8. Zhu, W. et al. Interaction between mitochondrial homeostasis and barrier function in lipopolysaccharide-induced endothelial cell injury. *Int J Exp Pathol.* **104**(6), 272–282 (2023).
9. Li, Z. et al. Xuanfei Baidu formula alleviates impaired mitochondrial dynamics and activated NLRP3 inflammasome by repressing NF-κB and MAPK pathways in LPS-induced ALI and inflammation models. *Phytomedicine: Int J Phytotherapy Phytopharmacology* **108**, 154545 (2023).
10. Zhao, N. et al. High concentration hydrogen mitigates Sepsis-Induced acute lung injury in mice by alleviating mitochondrial fission and dysfunction. *J Personalized Med.* **13**(2), 244 (2023).
11. Hernández-Cuervo, H. et al. BMI1 Silencing induces mitochondrial dysfunction in lung epithelial cells exposed to hyperoxia. *Front Physiol.* **13**, 814510 (2022).
12. Islam, M. N. et al. Mitochondrial transfer from bone-marrow-derived stromal cells to pulmonary alveoli protects against acute lung injury. *Nat Med.* **18**(5), 759–765 (2012).
13. Dutra Silva, J. et al. Mesenchymal stromal cell extracellular vesicles rescue mitochondrial dysfunction and improve barrier integrity in clinically relevant models of ARDS. *Eur Respir J.* **58**(1), 2002978 (2021).
14. Harijith, A. et al. NOX4 mediates epithelial cell death in hyperoxic acute lung injury through mitochondrial reactive oxygen species. *Front Pharmacol.* **13**, 880878 (2022).
15. Wilson, P. C. & Humphreys, B. D. Single-cell genomics and gene editing: implications for nephrology [J]. *Nat Rev Nephrol.* **15** (2), 63–64 (2019).
16. Ding, S., Chen, X. & Shen, K. Single-cell RNA sequencing in breast cancer: Understanding tumor heterogeneity and paving roads to individualized therapy. *Cancer communications.* **40**(8), 329–344 (2020).
17. Piwecka, M., Rajewsky, N. & Rybak-Wolf, A. Single-cell and Spatial transcriptomics: Deciphering brain complexity in health and disease. *Nat Reviews Neurol.* **19**(6), 346–362 (2023).
18. Ritchie, M. E. et al. Limma powers differential expression analyses for RNA-sequencing and microarray studies [J]. *Nucleic Acids Res.* **43** (7), e47 (2015).

19. Wu, T. et al. ClusterProfiler 4.0: A universal enrichment tool for interpreting omics data. *Innovation (Cambridge (Mass))*. **2**(3), 100141 (2021).
20. Hao, Y. et al. Integrated analysis of multimodal single-cell data. *Cell.* **184**(13), 3573–3587 (2021).
21. Lun, A. T., McCarthy, D. J. & Marioni, J. C. A step-by-step workflow for low-level analysis of single-cell RNA-seq data with bioconductor. *F1000Research*. **5**, 2122 (2016).
22. Hafemeister, C., Satija, R. & Normalization and variance stabilization of single-cell RNA-seq data using regularized negative binomial regression. *Genome Biol.* **20**(1), 296 (2019).
23. Wang, Z. et al. Healing mechanism of diabetic foot ulcers using single-cell RNA-sequencing [J]. *Annals Translational Med.* **11**(5), 210 (2023).
24. Simon, N. et al. Regularization paths for cox's proportional hazards model via coordinate descent. *J Stat Softw.* **39**(5), 1–13 (2011).
25. Hänzelmann, S., Castelo, R. & Guinney, J. GSVA: gene set variation analysis for microarray and RNA-seq data. *BMC Bioinform.* **14**, 7 (2013).
26. Chen, B. et al. Profiling Tumor Infiltrating Immune Cells with CIBERSORT.*Methods Mol Bio.* **1711**, 243–259 (2018).
27. Liu, X. S. et al. SLC2A1 is a diagnostic biomarker involved in immune infiltration of colorectal cancer and associated with m6A modification and CeRNA. *Front Cell Dev Biology* **10**, 853596 (2022).
28. Guo, W. et al. Elevated SLC2A1 expression correlates with poor prognosis in patients with surgically resected lung adenocarcinoma: A study based on immunohistochemical analysis and bioinformatics [J]. *DNA Cell Biol.* **39** (4), 631–644 (2020).
29. Yan, S. et al. Deregulated SLC2A1 promotes tumor cell proliferation and metastasis in gastric cancer. *Int J Mol Sci.* **16**(7), 16144–16157 (2015).
30. Min, K. W. et al. High SLC2A1 expression associated with suppressing CD8 T cells and B cells promoted cancer survival in gastric cancer [J]. *PloS One*. **16** (3), e0245075 (2021).
31. Oda, Y. et al. SLC2A1/GLUT1 expression in mural nodules of intraductal papillary mucinous neoplasm of the pancreas. *Hum Pathol.* **65**, 71–78 (2017).
32. Shang, R. et al. Long noncoding RNA SLC2A1-AS1 regulates aerobic Glycolysis and progression in hepatocellular carcinoma via inhibiting the STAT3/FOXM1/GLUT1 pathway. *Mol Oncol.* **14** (6), 1381–1396 (2020).
33. Hao, B. et al. Identification of SLC2A1 as a predictive biomarker for survival and response to immunotherapy in lung squamous cell carcinoma. *Comput Biol Med.* **171**, 108183 (2024).
34. Freemerman, A. J. et al. Metabolic reprogramming of macrophages: glucose transporter 1 (GLUT1)-mediated glucose metabolism drives a Proinflammatory phenotype. *J Biol Chem.* **289**(11), 7884–7896 (2014).
35. Nicita, F. et al. SLC2A1 mutations are a rare cause of pediatric-onset hereditary spastic paraplegia. *Eur J Paediatr Neurol.* **23**(2), 329–332 (2019).
36. Villanueva, C. E. & Hagenbuch, B. Palmitoylation of solute carriers. *Biochem Pharmacol.* **215**, 115695 (2023).
37. Rostami, M. R. & Bradic, M. The derepression of transposable elements in lung cells is associated with the inflammatory response and gene activation in idiopathic pulmonary fibrosis. *Mob DNA* **12**(1), 14 (2021).
38. Xu, N. et al. A Five-Genes based diagnostic signature for Sepsis-Induced ARDS. *Pathol Oncol Research: POR* **27**, 580801 (2021).
39. Jiang, Y. et al. Single cell RNA sequencing identifies an early monocyte gene signature in acute respiratory distress syndrome. *JCI Insight.* **5**(13), e135678 (2020).
40. Duan, C. et al. SARS-CoV-2 achieves immune escape by destroying mitochondrial quality: comprehensive analysis of the cellular landscapes of lung and blood specimens from patients with COVID-19. *Front Immunol.* **13**, 946731 (2022).
41. Jin, W., Jin, W. & Pan, D. Ifi27 is indispensable for mitochondrial function and Browning in adipocytes. *Biochem Biophys Res Commun.* **501**(1), 273–279 (2018).
42. Min, Z. et al. IFI27 as a potential indicator for severe enterovirus 71-infected hand foot and mouth disease [J]. *Virus Res.* **289**, 198149 (2020).
43. Yao, R. Q. et al. Single-cell transcriptome profiling of sepsis identifies HLA-DR(low)S100A(high) monocytes with immunosuppressive function. *Military Med Res.* **10**(1), 27 (2023).
44. Jain, K. et al. Reconditioned monocytes are Immunomodulatory and regulate inflammatory environment in sepsis. *Sci Rep.* **13**(1), 14977 (2023).
45. Mukherjee, R. et al. Non-Classical monocytes display inflammatory features: validation in sepsis and systemic lupus erythematous. *Sci Rep.* **5**, 13886 (2015).
46. Gainaru, G. et al. Increases in inflammatory and CD14(dim)/CD16(pos)/CD45(pos) patrolling monocytes in sepsis: correlation with final outcome. *Critical care.* **22**(1), 56 (2018).
47. Tao, P. et al. Investigating the Intercellular Communication Network of Immune Cell in Acute Respiratory Distress Syndrome with Sepsis. *Comput Math Methods Med* 4586648 (2022).
48. Cao, C. et al. Transcriptional characterization of Bronchoalveolar lavage fluid reveals immune microenvironment alterations in chemically induced acute lung injury. *J Inflamm Res.* **16**, 2129–2147 (2023).
49. Roux, M. et al. Plasma levels of hsa-miR-152-3p are associated with diabetic nephropathy in patients with type 2 diabetes. *Nephrol Dial Transplant.* **33** (12), 2201–2207 (2018).
50. Luo, Y. et al. Bioinformatics identification of potentially involved MicroRNAs in Tibetan with gastric cancer based on MicroRNA profiling [J]. *Cancer Cell Int.* **15**, 115 (2015).
51. Xu, Y. et al. Hsa-miR-140-5p down-regulates LDL receptor and attenuates LDL-C uptake in human hepatocytes. *Atherosclerosis.* **297**, 111–119 (2020).
52. López-Sánchez, G. N. et al. Hepatic mir-122-3p, mir-140-5p and mir-148b-5p expressions are correlated with cytokeratin-18 serum levels in MAFLD. *Ann Hepatol.* **27**(6), 100756 (2022).
53. Sun, F. et al. Exosomes derived from the blood of patients with sepsis regulate apoptosis and aerobic glycolysis in human myocardial cells via the hsa–miR–1262/SLC2A1 signaling pathway. *Mol Med Rep.* **25**(4), 119 (2022).
54. Kang, Y. J. MicroRNA-22 Regulates the Pro-inflammatory Responses and M1 Polarization of Macrophages by Targeting GLUT1 and 4-1BBL. *J Immunol Res*, 2457006 (2023).
55. Chen, M. et al. miRNA-206-3p alleviates LPS-induced acute lung injury via inhibiting inflammation and pyroptosis through modulating TLR4/NF-κB/NLRP3 pathway. *Sci Rep.* **14**(1), 11860 (2024).
56. Martins Freire, C. et al. Complete absence of GLUT1 does not impair human terminal erythroid differentiation [J]. *Blood Adv.* **8** (19), 5166–5178 (2024).
57. Liu, L. et al. The GLUT1-mTORC1 axis affects odontogenic differentiation of human dental pulp stem cells [J]. *Tissue Cell.* **76**, 101766 (2022).

Acknowledgements

We would like to thank Scribendi (https://www.scribendi.com/) for English language editing.

Author contributions

Huang Hongyuan and Chen Mengchi have made equal contributions to this paper. Huang Hongyuan and Chen Mengchi were responsible for the study's central conception and the manuscript draft. Huang Hongyuan collect-

ed clinical specimens, and Chen Mengchi carried out experiments. Liang Yingying and Huang Qiaojuan helped to design the study and performed the statistical analysis. Liu Jianghua and Zheng Xiaowen made the overall planning for this study and put forward constructive suggestions. All authors have read and approved the final manuscript.

Funding
1. Department of Science and Technology of Guangxi Zhuang Autonomous Region, Joint Special Project for Research on Regional High-Prevalence Diseases, Grant number: 2024GXNSFAA010113.
2. Department of Science and Technology of Guangxi Zhuang Autonomous Region, Joint Special Project for Research on Regional High-Prevalence Diseases, Grant number: 2023GXNSFAA026202.

Declarations

Competing interests
The authors declare no competing interests.

Ethical review approval
Approval for this study was obtained from the Ethics Committee of the Second Affiliated Hospital of Guangxi Medical University, No: 2024-KY (0512).

Disclosure statement
The authors declared no potential conflicts of interest with respect to the research, authorship, and/or publication of this article.

Additional information
Supplementary Information The online version contains supplementary material available at https://doi.org/10.1038/s41598-025-13448-8.

Correspondence and requests for materials should be addressed to L.J.

Reprints and permissions information is available at www.nature.com/reprints.

Publisher's note Springer Nature remains neutral with regard to jurisdictional claims in published maps and institutional affiliations.